Analytical Cellular Pathology / Cellular Oncology 33 (2010) 191–205
DOI 10.3233/ACP-CLO-2010-0538
IOS Press

Dual effects of β_3 integrin subunit expression on human pancreatic cancer models

S. Marchán [a], S. Pérez-Torras [a], A. Vidal [a], J. Adan [b,*], F. Mitjans[b,*], N. Carbó [a] and A. Mazo [a,**]
[a] *Departament de Bioquímica i Biologia Molecular, Institut de Biomedicina de la UB, Universitat de Barcelona, Barcelona, Spain*
[b] *Laboratori de Bioinvestigació, Merck Farma i Química, Barcelona, Spain*

Abstract. *Background:* Pancreatic cancer, the fifth leading cause of adult cancer death in Western countries, lacks early detection, and displays significant dissemination ability. Accumulating evidence shows that integrin-mediated cell attachment to the extracellular matrix induces phenotypes and signaling pathways that regulate tumor cell growth and migration.

Methods: In view of these findings, we examined the role of β_3 in pancreatic cancer by generating two stable β_3-expressing pancreatic human cell lines and characterizing their behavior *in vitro* and *in vivo*.

Results: Transduction of β_3 selectively augmented the functional membrane $\alpha_v\beta_3$ integrin levels, as evident from the enhanced adhesion and migration abilities related to active Rho GTPases. No effects on *in vitro* anchorage-dependent growth, but higher anoikis were detected in β_3-overexpressing cells. Moreover, tumors expressing β_3 displayed reduced growth. Interestingly, treatment of mice with an α_v-blocking antibody inhibited the growth of β_3-expressing tumors to a higher extent.

Conclusions: Our results collectively support the hypothesis that $\alpha_v\beta_3$ integrin has dual actions depending on the cell environment, and provide additional evidence on the role of integrins in pancreatic cancer, which should eventually aid in improving prediction of the effects of therapies addressed to modulate integrin activities in these tumors.

Keywords: Pancreatic cancer, integrins, cell migration, tumor growth, $\alpha_v\beta_3$

1. Introduction

Acquisition of enhanced ability to invade adjacent tissues and distant sites facilitates tumor progression towards increasingly malignant and aggressive phenotypes. The crossing of tissue barriers, a process necessary for metastasis, requires increased cell motility driven by remodeling of the cytoskeleton and cell contacts with the extracellular matrix [34,40].

Integrins play an important role in adhesive functions as well as modulation of different signal transduction pathways. These heterodimeric transmembrane receptors bind via their globular head domains to components of the extracellular matrix (ECM). The types of integrins present on the cell surface and nature of the ligands determine which signaling pathways are activated [16,18,25].

Activated signals may synergize to induce Rho GTP-Pase family proteins (Cdc42, Rac1 and RhoA), leading to cytoskeletal rearrangement and cell migration [33]. Rho proteins regulate the levels and timing of expression of a number of critical genes involved in the cell cycle, such as cyclin D_1, as well as interconnecting migration and proliferation processes. This leads to changes in cell cycle progression via modulation of cyclin D-CDK4/6 and cyclin E-CDK2 complex activities [9,39]. Interestingly, cell cycle regulators, such as p27, also regulate Rho signaling via direct binding and inactivation of RhoA [5]. On the other hand, under cell–ECM detachment conditions, specific integrins actively induce apoptosis-promoting signals, leading to a type of apoptosis termed 'anoikis' [15,41]. However, the mechanisms by which integrins switch from survival/migration to proapoptotic signals upon cell detachment from the substrate remain to be established. Changes in integrin expression patterns may subsequently determine cell fate via involvement in proliferation, migration and cell death processes [8, 36].

*Present address: Leitat Technological Center, Biomed Division.
**Corresponding author: Dr. Adela Mazo, Departament de Bioquímica i Biología Molecular, Facultat de Biologia, Universitat de Barcelona, Diagonal 645, 08028 Barcelona, Spain. Tel.: +34 934021210; Fax: +34 934021559; E-mail: amazo@ub.edu.

$\alpha_v\beta_3$, a vitronectin/RGD receptor, is a well characterized integrin expressed in both endothelial and cancer cells [35,42]. The $\alpha_v\beta_3$ integrin is overexpressed in various solid tumors, and correlates with increased invasiveness [3,40]. The contribution of $\alpha_v\beta_3$ to the invasive behavior of neoplastic cells may be explained by positive regulation of cell migration through the above relationship with Rho GTPases. However, $\alpha_v\beta_3$ integrin has also been involved in anoikis induction in several cell types [24,41], indicating functional promiscuity with wide implications in metastatic dissemination.

Surprisingly, mice lacking $\alpha_v\beta_3$ and $\alpha_v\beta_5$ integrins exhibited extensive, rather than decreased angiogenesis and tumor growth [32]. Elevated neovascularization in tumors is partly related to increases in Flk1/VEFGR2 signaling in endothelial cells of β_3-null mice [31], suggesting that $\alpha_v\beta_3$ integrin induces downregulation of VEGFR2 expression under specific conditions. Moreover, Taverna et al. [37] showed that $\alpha_v\beta_3$ and $\alpha_v\beta_5$ integrins are not essential for tumor growth, progression and metastasis of mammary carcinomas, thus providing further controversy regarding the role of this integrin in tumor development.

Recently, it has been reported that $\alpha_v\beta_3$ can act as mediator of anchorage independence, an action that is in accordance to the aggressive behaviour of integrin $\alpha_v\beta_3$-expressing human tumors [12,38] but in a clear discordance with and its involvement in anoikis and the results in KO mice.

In order to investigate the β_3 role in pancreatic cancer, we generated β_3-overexpressing human pancreatic cancer cells, and analyzed the effects of $\alpha_v\beta_3$ integrin on their behavior *in vitro* and *in vivo*. Our data show that high levels of the integrin are correlated with increased p27 expression, together with changes in the ratio of RhoA/Rac1 activities that favor cell migration. However, tumor growth was inhibited upon $\alpha_v\beta_3$ expression and treatment with an anti-α_v antibody. These results collectively present additional evidence in favor of the involvement of the cell environment in the dual roles of $\alpha_v\beta_3$ integrin.

2. Materials and methods

2.1. Cell lines, β_3 clone generation and culture conditions

NP-18 and NP-9 cell lines were derived from human pancreatic adenocarcinomas xenografted in nude mice [7] established at the Hospital de la Santa Creu i Sant Pau (Barcelona, Spain), and kindly provided by the Gastrointestinal Investigation Laboratory of the hospital.

NP-9β_3 and NP-18β_3 cell lines were obtained from parental NP-9 and NP-18, respectively, by stable transduction with a β_3 integrin subunit-containing retroviral vector. AM12 packaging cell lines transfected with the empty retroviral vector (pBabe) or human β_3 integrin cDNA-containing vector (pBabe/β_3) were kindly provided by Dr. John Marshall (St. Thomas Hospital, London). Briefly, AM12 conditioned culture media were used to infect exponentially growing NP-9 and NP-18 cells. At 24 h after transduction, culture medium was replaced with puromycin-containing medium for transfectant cell selection. Cell cloning was performed by limit dilution, and several isolated clones were obtained and further characterized. Parental and β_3-expressing NP-18 cells (cultured in RPMI-1640 medium) and NP-9 cells (cultured in DMEM:F12 medium) were maintained at 37°C in a humidified atmosphere with 5% CO_2. All media contained 10% fetal calf serum and Penicillium/Streptomycin as antibiotics. Under maintenance conditions, 1.25 μg/ml puromycin was added to all transfectants culture media but it was eliminated during the experiments.

In cell cultures grown under anchorage-independent conditions, six-well plates were coated with the non-adhesive substrate, poly-HEMA (10 mg/ml in 95% ethanol), at 3 ml/well. Next, 5×10^5 cells/well were plated and incubated for 4 days (NP-18/NP-18β_3) or 7 days (NP-9/NP-9β_3) under the above culture conditions. Cells were gently recovered, and subjected to apoptosis detection and cell cycle analysis.

2.2. Cell growth analysis and volume calculation

To determine growth curves, 2,500 cells/well (for NP-18, NP-18β_3 and NP-9β_3), or 5,000 cells/well (for NP-9) were seeded in 24-well tissue plates. Quadruplicate wells were counted daily from days 1–8 after seeding. Cell number and volume were assessed in a Multisizer auto-analyzer (Coulter Corp., Hialechm, FL, USA). Data were plotted semilogarithmically. The slope at the linear segment was calculated, and used for doubling time estimation (h) using the equation: Ln(2) × 24 h/slope.

2.3. Adhesion assays

For these experiments, 96-well dishes (Dynatech, Chantilly, VA, USA) were coated with several concentrations of human plasma vitronectin (VN) (Collaborative Biomedical Products, Bedford, MA, USA) or human plasma fibrinogen (FB) (Sigma-Aldrich, St. Louis, MO, USA) and incubated at 4°C overnight. Immediately after blockage with 1% BSA, 50,000 cells (control and mock-transfected NP-9 and control, mock- and β_3-transfected NP-18) and 25,000 cells (NP-9β_3) in adhesion medium (RPMI-1640 or DMEM:F12 with 1% Bovine Serum Albumin (BSA)) were added to each well and incubated at 37°C. After 1 h, unattached cells were removed by rinsing with PBS, and the remaining attached cells fixed in 2% formaldehyde. Cells were stained with 0.1% crystal violet. Following washing and drying of cells, color was developed with 0.1 M HCl, and read on a microtiter plate spectrophotometer at 630 nm.

For inhibition of cell adhesion assays, serial dilutions of anti-α_v 17E6 and anti-$\alpha_v\beta_3$ LM609 antibodies (kindly provided by Merck) were added to the adhesion medium in VN (2 μg/ml for NP-9/NP-9β_3 and 1 μg/ml for NP-18/NP-18β_3 cells) or FB-coated dishes (15 μg/ml for NP-9β_3 and 10 μg/ml for NP-18β_3 cells). The percentage of cell adhesion inhibition was calculated, taking the value of control wells without antagonist as 100% adhesion.

2.4. Migration assays

For wounding migration assays, cells were plated at a high density on 24 mm glass coverslips. After 24 h, confluent cultures were wounded using a blue pipette tip, washed twice to remove unattached and damaged cells, and incubated overnight in fresh culture medium covered with mineral oil at 37°C and 5% CO_2. Phase-contrast images were obtained every 15 min with a 10× dry lens on a Widefield CCD System (Carl Zeiss MicroImaging Inc., Jena, Germany). Images were subsequently analyzed using ImageJ software (NIH, Bethesda, MD, USA), and migration speed calculated as net displacement (μm)/time (h).

For transwell assays, both sides of Fluoroblock Transwell Filters (8 μm) were coated with purified VN at a concentration of 15 μg/ml. Cells were suspended in basal medium containing 1% BSA. Samples consisting of 30,000 cells for NP-9 and NP-9β_3 and 50,000 cells for NP-18 and NP-18β_3 were plated on each filter. Migration was induced by adding 400 μl of medium supplemented with 1% BSA and 50 μg/ml of hepatocyte growth factor (HGF) to the feeder well. Filters were placed into 24-well dishes, and incubated for 6 h (NP-9/NP-9β_3) or 12 h (NP-18/NP-18β_3). For inhibition of cell migration, anti-$\alpha_v\beta_3$ LM609 antibody was added to the migration medium (100 μg/ml). Individual conditions were analyzed in triplicate. Fifteen minutes before the end of the assay, calcein-AM was added to feeder wells at a final concentration of 5 μM. Filters were examined using fluorescence microscopy and the fluorescence lecture was made with the Cytofluor 2300 System (Applied Biosystems, Carlsbad, CA, USA)

2.5. Flow cytometry

Cells were trypsinized, harvested in culture medium, and washed with PBS. Aliquots of cells (10^6) were incubated with each primary antibody for 20 min at 4°C. After washing with PBS-1% BSA, cells were incubated with FITC-conjugated secondary antibodies (Molecular Probes) for 30 min at 4°C. Cells were resuspended in PBS-containing propidium iodide (5 μg/ml) prior to flow cytometric analysis. Living cells were gated on the basis of their side and forward scatter and propidium iodide fluorescence. The following mAbs were used: AP3 for β_3, 11D1 for β_5, P4C10 for β_1, 5C4 for β_6, 17E6 for α_v, and LM609 for $\alpha_v\beta_3$ (all kindly provided by Merck) and 14e5 for β_8 (kindly provided by Dr. Stephanie Cambier).

To analyze the cell cycle profiles, culture cells were harvested at different times after seeding, fixed in 70% ice-cold ethanol, washed with ice-cold PBS, and stained in Tris-buffered saline containing propidium iodide (50 μg/ml), RNase A (10 μg/ml) for 1 h at 4°C. In all cases, data from >10,000 cells were collected and analyzed using WinMDI/Multicycle software (Phoenix Flow Systems, San Diego, CA, USA).

All measurements were performed on Epics XL (Coulter Corp., Hialechm, FL, USA) or Elite (Coulter Corp., Hialechm, FL, USA) flow cytometers.

2.6. Immunofluorescence

Cells were seeded on 10 mm glass coverslips. After 24 h, cells were washed twice in PBS, fixed in 4% paraformaldehyde for 30 min, washed again and permeabilized in 0.2% Triton X-100 for 5 min. After 1 h of blocking with 3% BSA in PBS at room temperature, cells were incubated with primary antibodies at room temperature for 1 h (anti-paxillin and anti-p27 (Transduction Laboratories, Lexington,

KY, USA) anti-CDK1 (Santa Cruz Biotechnology Inc., Santa Cruz, CA, USA) and anti-$\alpha_v\beta_3$, clone 23C6 (gently given by Dr. Erik Danen). Next, cells were washed three times with PBS, and coverslips incubated at room temperature for 1 h in the dark with FITC-conjugated anti-mouse immunoglobulins (Jackson ImmunoResearch, Newmarket Suffolk, England) and Texas Red (TR)-conjugated Phalloidin (Molecular Probes, Eugene, OR, USA) for actin staining. All antibodies were diluted in washing solution containing 0.5% BSA and 0.005% saponin in PBS. Mowiol 4-88 solution supplemented with DABCO (Calbiochem, La Jolla, CA, USA) was employed as mounting medium. Photomicrographs were obtained with a confocal Leica TCS NT microscope (Leica Microsystems, Wetzlan, Germany) using a 63× oil objective.

2.7. Western blot analysis

Cells were lysed in 10 mM Tris-HCl (pH = 7.4), 400 mM NaCl, 5 mM NaF, 10% glycerol, 1 mM EDTA, 1 mM Na_3VO_4, 0.5% Igepal CA-630, 4 mM DTT supplemented with protease inhibitor cocktail (Roche, Mannheim, Germany). Protein concentration was determined using the Bradford (Bio-Rad) assay. Total protein (40 μg) was electrophoresed on SDS-polyacrylamide gels (8–12%). For integrin determination, non-reducing conditions were used. Proteins were electrotransferred to nitrocellulose membranes (Schleicher and Schuell, Dassel, Germany) and probed with the following specific primary antibodies: the above mentioned anti-β_6(5C4) and anti-β_3 (AP3), anti-β_8(3/8) (kindly provided by Stephanie Cambier), anti-$CycD_1$ (SC-8396), anti-CycE (HE12), anti-CycA (C-19), anti-p21 (C-20), anti-p27 (C-19), anti-CDK6 (C-21), anti-CDK4 (H22), anti-CDK2 (M2) and anti-CDK1 (SC-54) (Santa Cruz Biotechnology Inc., Santa Cruz, CA, USA), anti-p16 (13251A) and anti-PARP (7D3-6) (Pharmingen, San Diego, CA, USA), and anti-actin (A2066) (Sigma-Aldrich, St. Louis, MO, USA). After washing, membranes were incubated with corresponding HRP-conjugated anti-mouse IgG (DAKO, Carpinteria, CA, USA) and anti-rabbit IgG (Sigma-Aldrich, St. Louis, MO, USA) secondary antibodies. The blot was developed using the enhanced chemiluminescence detection system (Amersham, Arlington Heights, IL, USA).

2.8. Rho/Rac–GTPase activity

Cells growing subconfluently on 14 mm dishes in standard medium were lysed with 1 ml Nonidet P-40 lysis buffer (50 mM Tris-HCl, pH 7.4, 100 mM NaCl, 1% Nonidet P-40, 10% glycerol, 10 mM $MgCl_2$) supplemented with protease inhibitor mix (1:1000) (Sigma-Aldrich, St. Louis, MO, USA). Lysates were clarified by centrifugation at 14,000 rpm for 20 min at 4°C. A 1% aliquot was removed for determination of the total GTPase level. Clarified lysates were incubated for 45 min at 4°C with a GST fusion protein containing the Rho-binding domain of Rhotekin (a Rho effector protein) [29] or 30 min at 4°C with a biotinylated peptide corresponding to the Cdc42/Rac interactive binding motif in PAK1B (kindly provided by Dr. J. Collard). Complexes were bound to glutathione- or streptavidin-conjugated beads, and washed three times in Nonidet P-40 lysis buffer. Samples were analyzed using 14% SDS-PAGE, followed by Western blotting using RhoA (clone 26C4, Santa Cruz Biotechnology, Santa Cruz, CA, USA) and Rac1 (clone 102, Transduction Laboratories, Lexington, KY, USA) as primary antibodies. Finally, blots were processed according to previous reports to detect bound activated (GTP-loaded) and total GTPases.

2.9. In vivo assays

For subcutaneous (sc) tumors, a total of 12×10^6 (NP-9/NP-9β_3) or 5×10^6 (NP-18/NP-18β_3) tumor pancreatic cells were injected subcutaneously into each posterior flank region of BALB/c nude mice. For intrapancreatic (ip) tumor generation, mice were anesthetized by intraperitoneal injection of a ketamine/xylazine mixture (3:1). Subsequently, a small left flank laparotomy was made, and the tail of the pancreas and spleen carefully exposed. A 10 mg fragment from sc NP-18 or NP-18-β_3 tumors was fixed to the pancreas with a non-absorbable surgical suture (Prolene 5–0), the pancreas and spleen returned to the abdominal cavity, and the peritoneum and abdominal wall were closed with a surgical staple. Tumors were allowed to grow for 20 days (sc) or 5 weeks (ip). To determine the effects of the α_v-blocking antibody 17E6, at 24 h (sc tumors) or one week (ip tumors) after implantation, mice were randomly distributed into several treatment groups, specifically, controls receiving saline only and 17E6-treated mice receiving intraperitoneal injections (1 mg/mouse three times/week for 7 weeks (sc tumors) or 500 μg/mouse three times/week for 6 weeks (ip tumors)). In all assays, mice were sacrificed, following which tumors were removed and weighed.

All animal work was performed in compliance with the guidelines and approval of the Institutional Animal Care Committee.

2.10. Statistical analysis

Statistical analysis was performed using GraphPad Prism 4 software. p-values were calculated according to two-sided Student's t-test for independent samples and two-way ANOVA with Bonferroni correction.

3. Results

3.1. Integrin levels in β_3-overexpressing cells

To analyze the effects of $\alpha_v\beta_3$ integrin on human pancreatic cancer cells, we transduced two cell lines, NP-9 (weakly expressing β_3) and NP-18 (β_3-deficient), with a retroviral vector containing human β_3 integrin cDNA. One clone from each parental cell line overexpressing β_3 were selected (NP-9β_3 and NP-18β_3). NP-9β_3 displayed higher β_3 expression levels than NP-18β_3, as assessed by western blotting (Suppl. Fig. 1A: http://www.qub.ac.uk/isco/JCO) and FACS (Fig. 1A). Proper membrane localization of the $\alpha_v\beta_3$ dimer was confirmed in both cell lines with FACS analysis (Fig. 1A).

We additionally analyzed plasma membrane localization of other integrins closely related to β_3. Both parental cell lines were clearly positive for β_1 and β_5 subunits (Fig. 1B). In contrast, low levels of β_6 and β_8 subunits were detected solely in NP-9 cells (data not shown). We observed increased α_v subunit surface levels in both β_3-overexpressing cell lines (Fig. 1B), but no significant differences in the overall levels of β_5 (Fig. 1B), and β_6 and β_8 were obtained in any model (data not shown). Interestingly, a significant increase in the β_1 integrin subunit was observed in NP-18β_3 (Fig. 1B). This increase was accompanied by an additional 30% of the $\alpha_5\beta_1$ dimer in plasma membrane (data not shown).

3.2. Morphological features

Overexpression of β_3 induced marked morphological changes in NP-9β_3 cells, which showed a flattened and enlarged shape, compared to the parental cell line (Fig. 2). Moreover, the cell volume of NP-9β_3 was increased 1.7 $\pm$ 0.2-fold, compared to NP-9 (Table 1). Actin cytoskeleton and focal adhesion contacts were visualized by staining of actin and paxillin, respectively (Fig. 2A). Actin stress fibers and paxillin in focal adhesions were increased in NP-9β_3 cells, in keeping with the morphological changes induced by β_3. In NP-18β_3, less cortical actin was present, but distribution and number of focal adhesions were altered in a similar manner to that in NP-9β_3, even though cell shape and volume remained practically unaltered. The $\alpha_v\beta_3$ integrin was localized in structures resembling focal adhesion contacts in both cell lines, displaying typical clustering (Fig. 2B, Suppl. Fig. 1B: http://www.qub.ac.uk/isco/JCO).

3.3. Adhesion on specific matrices

Adhesion assays on specific coats demonstrated the functionality of newly synthesized β_3 dimers. As shown in Fig. 3A, while both parental and β_3-expressing cells bound vitronectin (VN), only the latter cells were able to interact at low VN concentrations. To confirm the role of $\alpha_v\beta_3$ integrin in enhanced adhesion ability to VN, inhibition adhesion assays with α_v- and $\alpha_v\beta_3$-blocking antibodies (17E6 and LM609, respectively) were performed (Fig. 3A). In all models, 17E6 cell adhesion was almost completely blocked on VN. Besides, cellular adhesion to VN was weakly (NP-9) or even not affected (NP-18) by LM609, according to the low (NP-9) or null (NP-18) $\alpha_v\beta_3$ basal expression in these cells. In contrast, NP-9β_3 and NP-18β_3 cell attachment to VN was partly abrogated by LM609 antibody, unveiling the contribution of $\alpha_v\beta_3$ integrin to the enhanced adhesion ability to VN displayed by these cells lines. Similar assays were performed on fibrinogen (FB). In this case, only β_3-overexpressing cells were able to bind the FB coating, verifying the functionality of ectopic $\alpha_v\beta_3$. As expected, inhibition adhesion assays with 17E6 on FB revealed complete abrogation of binding in both β_3-expressing cell lines (Fig. 3B).

3.4. Cell migration

The effects of β_3 on cell migration were initially analyzed using wound healing assays. Mean migration velocities were calculated for all cell lines. A β_3-induced stimulatory effect on migration was evident for NP-9β_3, which displayed fastest migration, compared with the other cell lines. Surprisingly, NP-18 and NP-18β_3 displayed similar migration velocities, suggesting that β_3 has no significant influence on the migratory behavior of NP-18 cells under these conditions (Fig. 4A). In migration assays performed on VN-coated transwells using HGF as a chemoattrac-

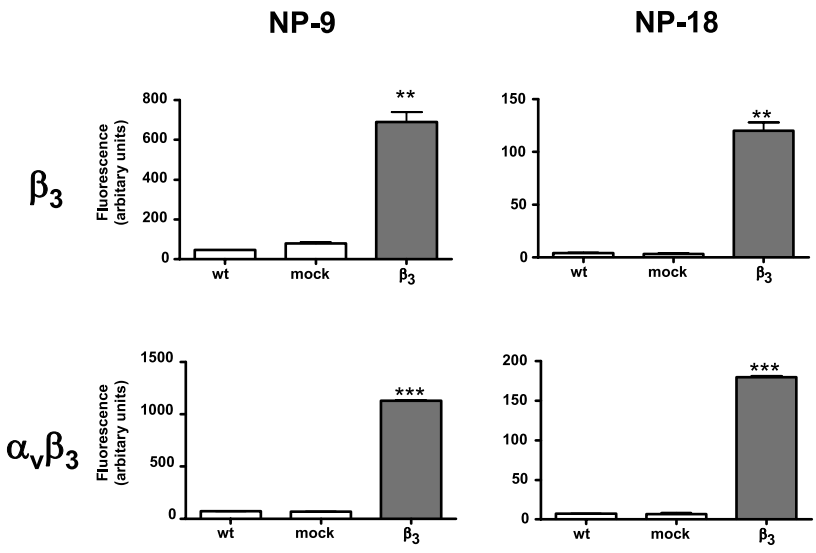

(A)

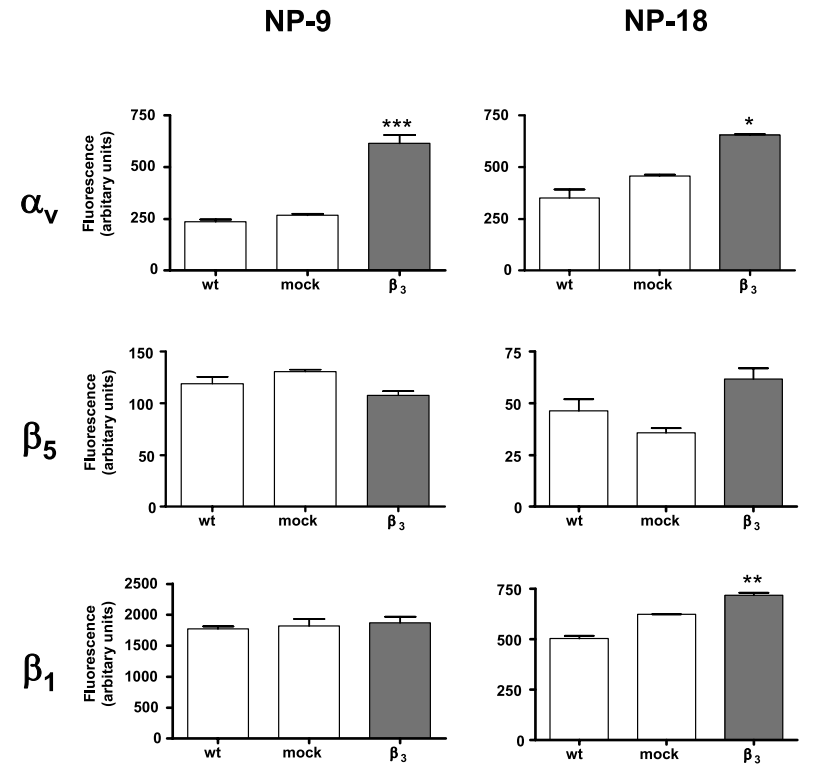

(B)

Fig. 1. Membrane presence of several integrin subunits and $\alpha_v\beta_3$ in NP-9 and NP-18 cell models. Cells were incubated with mAbs against β_3 (AP-3), $\alpha_v\beta_3$ (LM609), α_v (17E6), β_5 (P1F6) and β_1 (P4C10), followed by staining with FITC-conjugated rabbit anti-mouse Ig antibody, and analyzed using an Epics-XL flow cytometer. Bars depict fluorescence intensity for the different cell lines (wt: parental, mock: mock-transfected and β_3 : β_3-transfected). Means $\pm$ SD fluorescence units of three independent experiments are shown. Statistics: t-test, $^*p \leqslant 0.05$, $^{**}p \leqslant 0.01$, $^{***}p \leqslant 0.001$ vs. wt.

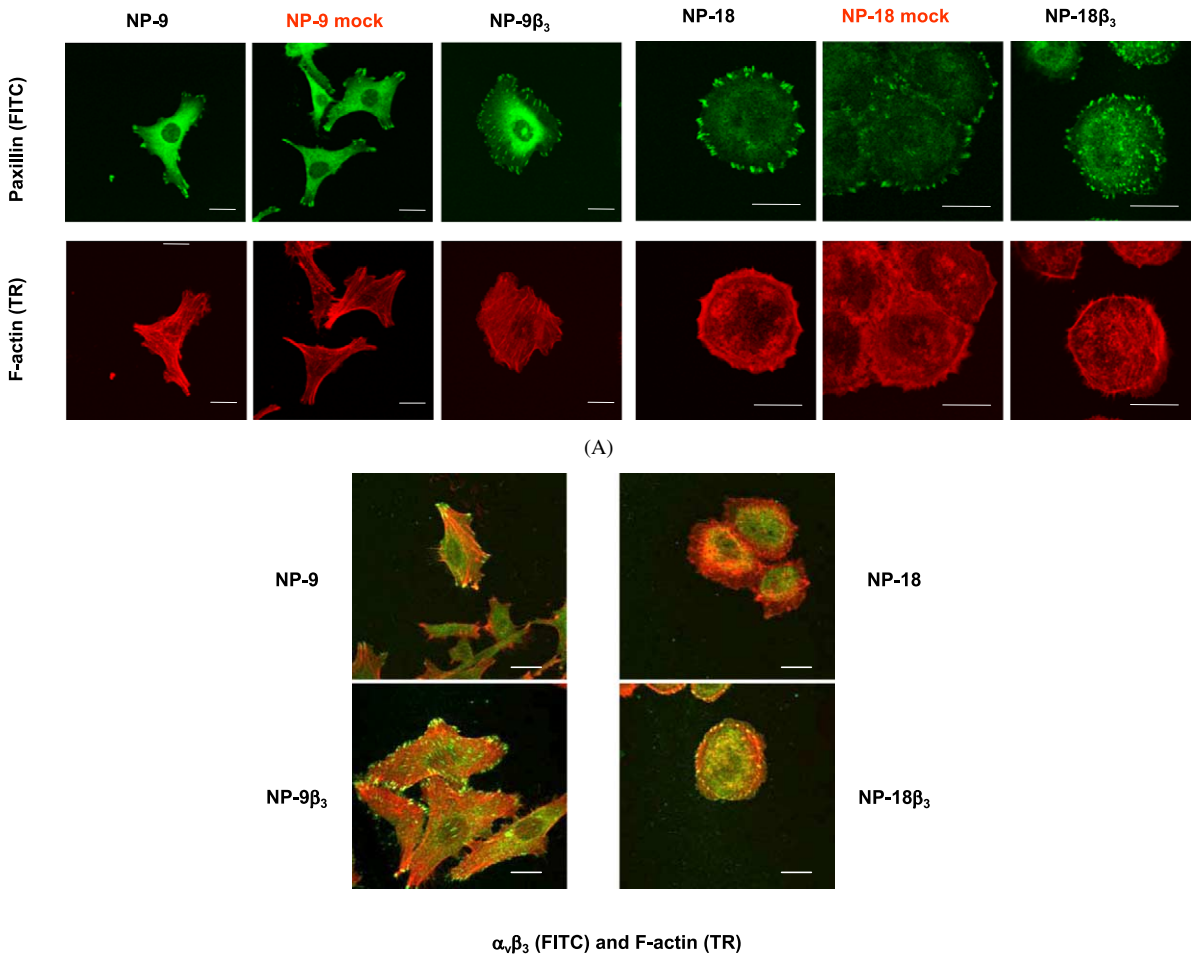

Fig. 2. Effects of β_3 overexpression on cell morphology. Cells (wt: parental, mock: mock-transfectants and β_3: β_3-transfectants) were grown in complete medium for 1 day on glass coverslips, fixed, permeabilized and stained for: (A) paxillin (FITC) and F-actin (TR), and (B) $\alpha_v\beta_3$ integrin (FITC) and F-actin (TR). All samples were analyzed using confocal microscopy. Bars, 20 μm.

Table 1
Effects of β_3 overexpression on cell volume

	Cell volume ± SD (μm^3)	
Cell line	NP-9	NP-18
wt	1694 ± 31	2179 ± 44
mock	1680 ± 16	2360 ± 46
β_3	2888 ± 16	2162 ± 24

Notes: Cell volume was assessed in a Multisizer auto-analyzer (Coulter Corp., Hialechm, FL, USA). The results are expressed in μm^3 as means ± SD of one representative experiment.

tant (Fig. 4B), both NP-9β_3 and NP-18β_3 cells showed higher migratory abilities than their corresponding parental cells. Positive correlation between $\alpha_v\beta_3$ levels and migration was observed in view of the finding that NP-9β_3 displayed the highest migration. To confirm the role of $\alpha_v\beta_3$ integrin in migration ability, assays on VN-coated transwells, in presence of the $\alpha_v\beta_3$-blocking antibody LM609 were performed. This specific antibody inhibited significantly cell migration of NP-18β_3 cells but did not affect cell migration of $\alpha_v\beta_3$ null NP18 cells (Fig. 4C).

3.5. *Rho GTPase activities*

Considering the involvement of GTPases of the Rho family in cell migration capacity, RhoA and Rac1 activities were analyzed using pull-down assays in all four models grown under standard conditions. Rac1-GTP levels were not altered in β_3-overexpressing cells. However, the RhoA-GTP level was diminished in NP-9β_3 cells, in accordance with their enhanced migration capacity observed in wound healing assays (Fig. 4D).

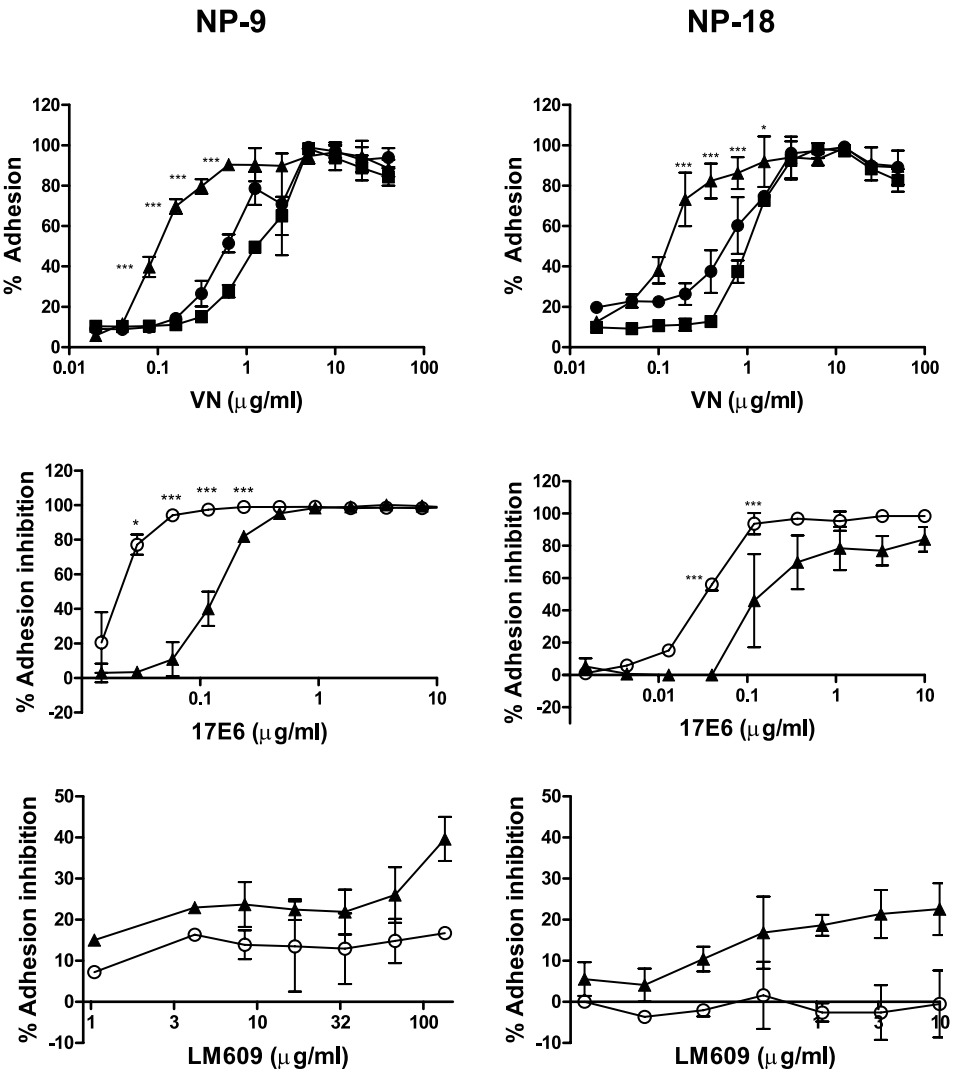

(A)

Fig. 3. Cell adhesion and adhesion inhibition assays. (A) Vitronectin (VN). For adhesion assays, results are presented as % of the maximum OD value of crystal violet-stained cells, working with sample triplicates in each experiment ($n = 3$). Symbols represent the following cell lines: (●) wt, (■) mock, and (▲) β_3-transfected. For adhesion inhibition assays, purified monoclonal antibodies (mAb) against α_v (17E6) or $\alpha_v\beta_3$ (LM609) were co-incubated during cell attachment to VN-coated substrates. Symbols represent the following conditions: (°) wt 17E6/LM609; (▲) β_3 17E6/LM609. Data are expressed as a percentage of cell adhesion inhibition. In all cases, means ± SD are shown. Statistics: 2-way ANOVA, $*p < 0.05$, $**p \leqslant 0.01$, $***p \leqslant 0.001$ vs. wt or mock.

3.6. Cell proliferation

The expression levels of several proteins involved in cell cycle progression were analyzed by western blotting to evaluate the possible effects of β_3 on cell proliferation. Among the proteins analyzed, increased levels of p27 and CDK1 were observed in NP-9β_3, compared with NP-9 cells. However, β_3 overexpression induced an increase in endogenous p16 levels in NP-18β_3 (Fig. 5A). No major changes in cell cycle profiles were evident between β_3 and parental cells (Fig. 5A). Moreover, doubling times were not significantly altered in β_3-overexpressing cell lines (44.6 ± 2.5 and 39.08 ± 0.6 h for NP-9 and NP-9β_3; 27.9 ± 0.5 and 25.3 ± 1 h for NP-18 and NP-18β_3, respectively).

Given that p27 and CDK1 play different roles depending on their subcellular localization, their presence was assessed using immunocytochemistry. p27 was localized mainly in the cytoplasm of the major-

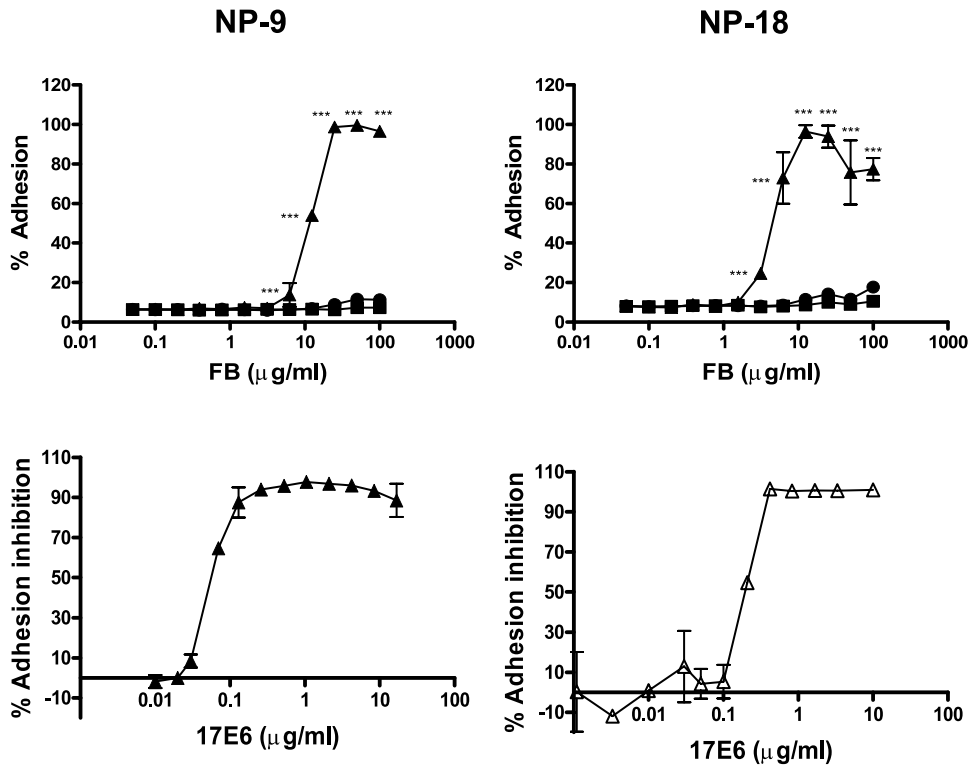

(B)

Fig. 3. (B) Fibrinogen (FB). For adhesion assays, results are expressed as % of the maximum OD value of crystal violet-stained cells, working with sample triplicates in each experiment ($n = 3$). Symbols: (●) wt; (■) mock and (▲) β_3-transfected. For adhesion inhibition assays, purified 17E6 mAb was co-incubated during cell attachment to fibrinogen-coated substrate. Symbols: (Δ) NP-9β_3 and (▲) NP-18β_3. In all cases, means ± SD are shown. Statistics: 2-way ANOVA, $^*p < 0.05$, $^{**}p \leqslant 0.01$, $^{***}p \leqslant 0.001$ vs. wt or mock.

ity of NP-9 and NP-9β_3 cells, displaying a diffuse distribution with clear intensification at the rear of cells. Immunofluorescence analysis revealed that CDK1 was ubiquitously expressed in both, the nucleus and cytoplasm, as well as in the cellular periphery. We observed no significant differences in the p27 or CDK1 distribution patterns between NP-9 and NP-9β_3 cells (Fig. 5A).

Cell cycle distribution of cultures in anchorage-independent conditions (poly-HEMA) was additionally analyzed. Under these conditions, all cell lines showed marked G_1 arrest and decrease in the S phase of the cell cycle. Moreover, a sub-G_1 population was observed, indicative of anoikis (Fig. 5B). Interestingly, this sub-G_1 population was more evident in both β_3 models than in the parental cell lines. Detection of PARP cleavage with Western blotting corroborated the induction of apoptosis under anchorage-independent culture conditions upon $\alpha_v\beta_3$ overexpression (Fig. 5B).

3.7. Tumor growth

To ascertain whether the changes observed *in vitro* are associated with differential growth *in vivo,* subcutaneous and intra-pancreatic tumors were generated by inoculation of β_3-overexpressing and corresponding parental cell lines. Comparison of tumor weights provided evidence that $\alpha_v\beta_3$ overexpression provokes growth-suppressive effects in both NP-9 and NP-18 subcutaneous models (Fig. 6A). The results obtained with orthotopic inoculation of NP-18 and NP-18β_3 indicate that this effect is independent of tumor location (Fig. 6B).

We further investigated the effects of the α_v-blocking antibody 17E6, on the growth of both subcutaneous and orthotopic tumors, using NP-18 and NP-18β_3 models. Surprisingly, while the contribution of $\alpha_v\beta_3$ integrin to growth was negative, blocking of α_v integrins reduced tumor growth to a higher extent in a manner dependent on β_3 expression levels (Figure 6C and D).

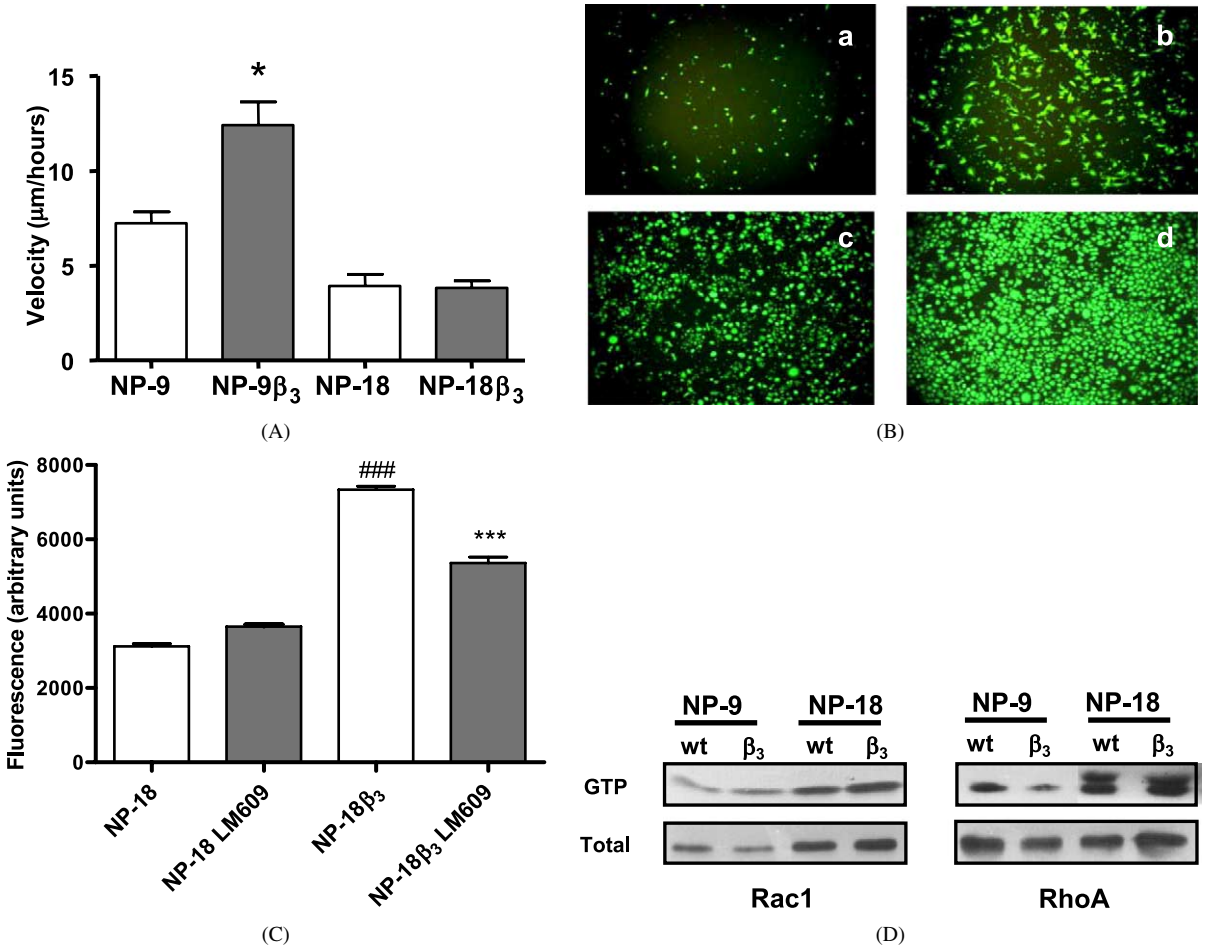

Fig. 4. Migration assays and small G protein activity. (A) Wound healing experiments. Cells were grown under standard conditions to confluence and artificially wounded by disrupting the monolayer with a sterile pipette. Migration velocities were determined using a Widefield CCD System. Bars depict means ± SD migration velocity of two different assays. Statistics: *t*-test, $*p \leqslant 0.05$. (B) Transwells assays. Cells were grown on VN-coated transwells and HGF was used as chemoattractant. Microphotographs (10×) were taken at 4 h for NP-9 (a) and NP-9β_3 (b) and at 12 h for NP-18 (c) and NP-18β_3 (d). A representative assay of three is shown. (C) For migration inhibition assays, purified LM609 mAb was co-incubated during cell migration. Statistics: *t*-test, $***p \leqslant 0.001$ vs. control and $^{\#\#\#}$ vs. parental cell line. (D) Rac1 and RhoA activation status. Active cellular RhoA and Rac1 were affinity-precipitated from lysates of cells grown under standard conditions using GST-C21 and PAK-CRIB-coated agarose beads, respectively. Total and active forms were detected by Western blotting using the corresponding antibodies. A representative immunoblot is shown. (Colors are visible in the online version of the article; http://dx.doi.org/10.3233/ACP-CLO-2010-0538.)

4. Discussion

Overexpression of $\alpha_v\beta_3$ integrin has been demonstrated in different human cancer cells, and correlates with increased invasive behavior in many solid tumor types [40]. Moreover, combination therapies, including integrin antagonists and others (such as signaling pathway inhibitors or radiotherapy) show that inhibition of $\alpha_v\beta_3$ integrin signaling enhances the antiangiogenic and antitumor effects elicited by other treatment regimes [1,6,20]. However, the stimulatory role of $\alpha_v\beta_3$ integrin in tumor formation was challenged, based on observations of increased angiogenesis in KO mice for $\alpha_v\beta_3$ or $\alpha_v\beta_5$ and $\alpha_v\beta_3$ integrins [32]. Additional evidence indicates that tumor growth and experimental metastasis are reduced upon $\alpha_v\beta_3$ overexpression, highlighting a dual role of $\alpha_v\beta_3$ integrin in angiogenesis and tumor growth [11,22].

While $\alpha_v\beta_3$ overexpression is not a common feature in PDAC, several investigators have linked expression of this integrin in endothelial and pancreatic cancer cells with enhanced vascularization, tumor growth, and invasiveness [13,17,19]. In an attempt to clarify the role of this integrin in pancreatic cancer behav-

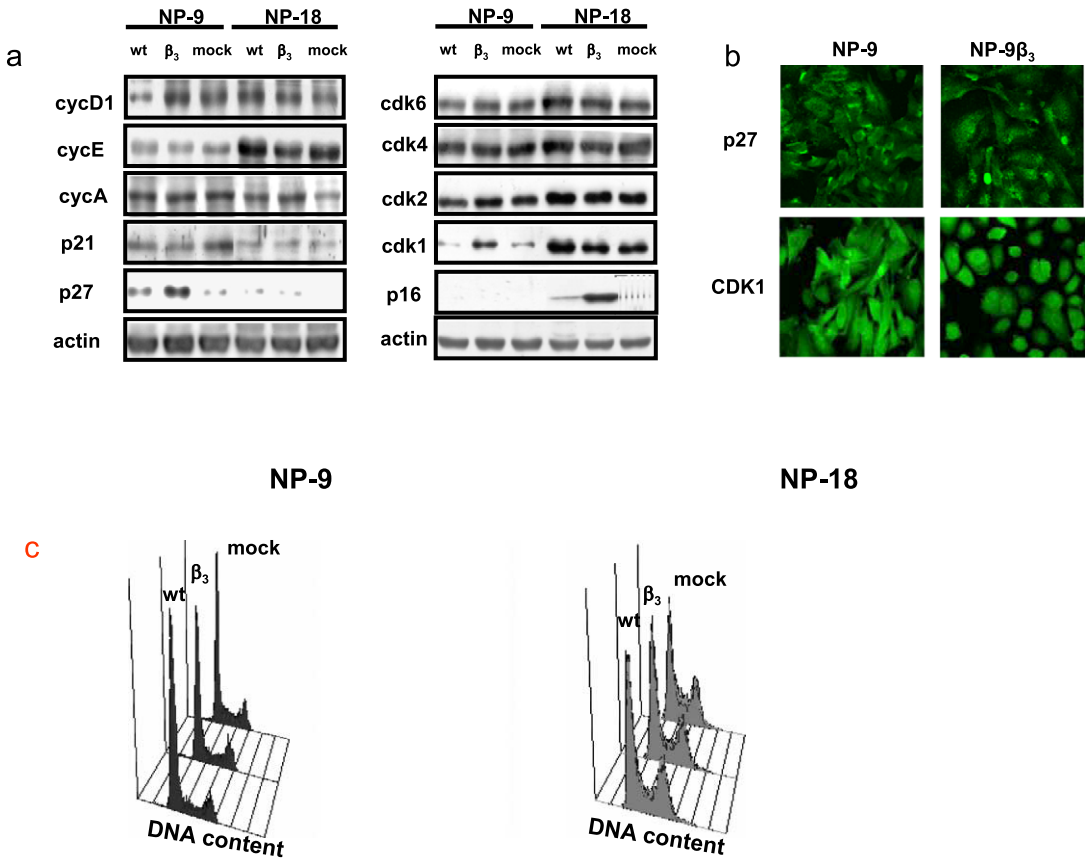

(A)

Fig. 5. Cell cycle and apoptosis analysis. (A) (a) Expression levels of cell cycle-related proteins. Two days after seeding, 40 μg of total protein extracts were immunoblotted using antibodies against different proteins involved in cell cycle progression. wt: parental, mock: mock-transfected and β_3: β_3-transfected. (b) Subcellular localization of p27 and cdk1 in NP-9 and NP-9β_3. Cells were grown for 1 day on glass coverslips in complete medium. Afterwards, cells were fixed, permeabilized and stained for p27 and CDK1 using FITC-conjugated anti-mouse IgG as secondary antibody. Samples were analyzed by fluorescence microscopy (×400). (c) Cell cycle profile. Cell cycle distribution was assessed by flow cytometry analysis of propidium iodide-stained cells during the exponencial phase of growth. wt: parental, mock: mock-transfectants and β_3: β_3-transfectants. (Colors are visible in the online version of the article; http://dx.doi.org/10.3233/ACP-CLO-2010-0538.)

ior, we generated and characterized two β_3-expressing pancreatic cancer cell lines, specifically, NP-9β_3 and NP-18β_3. In both cell lines, $\alpha_v\beta_3$ dimers were localized in focal adhesion contacts. Their functionality was demonstrated both, by the enhancement of the adhesion ability and cell migration on VN and the inhibitions elicited by specific antibodies.

Plasma membrane profiling of other β subunits closely related to β_3 was also monitored to clarify the extent to which the observed changes were directly related to β_3 subunit overexpression. No significant differences in the overall levels of other α_v partners were evident, with a slight increase in only β_1 levels in NP-18β_3. This finding may be related to the previously described cross-talk between β_1 and α_v integrins through which $\alpha_v\beta_3$ and $\alpha_v\beta_5$ surface levels are diminished upon β_1 expression [30]. Moreover, Danen et al. [10] further confirmed the β_1-mediated control of β_3 levels, and related this event to redistribution of focal contacts. It is possible that the β_1 increase observed in NP-18β_3 merely reflects a cellular response against β_3 overexpression and explains the mild β_3-overexpressing phenotype of this cell line, which correlates with the maintenance of cell morphology.

Interestingly, transcriptional upregulation of $\alpha_5\beta_1$ induced by p16 has been described in earlier reports [27,28]. Moreover, other studies show that overexpression of p16 inhibits migration of different tumor cells by controlling cell–cell and cell–ECM interactions through $\alpha_v\beta_3$ [2,4,14]. In this sense, the expected

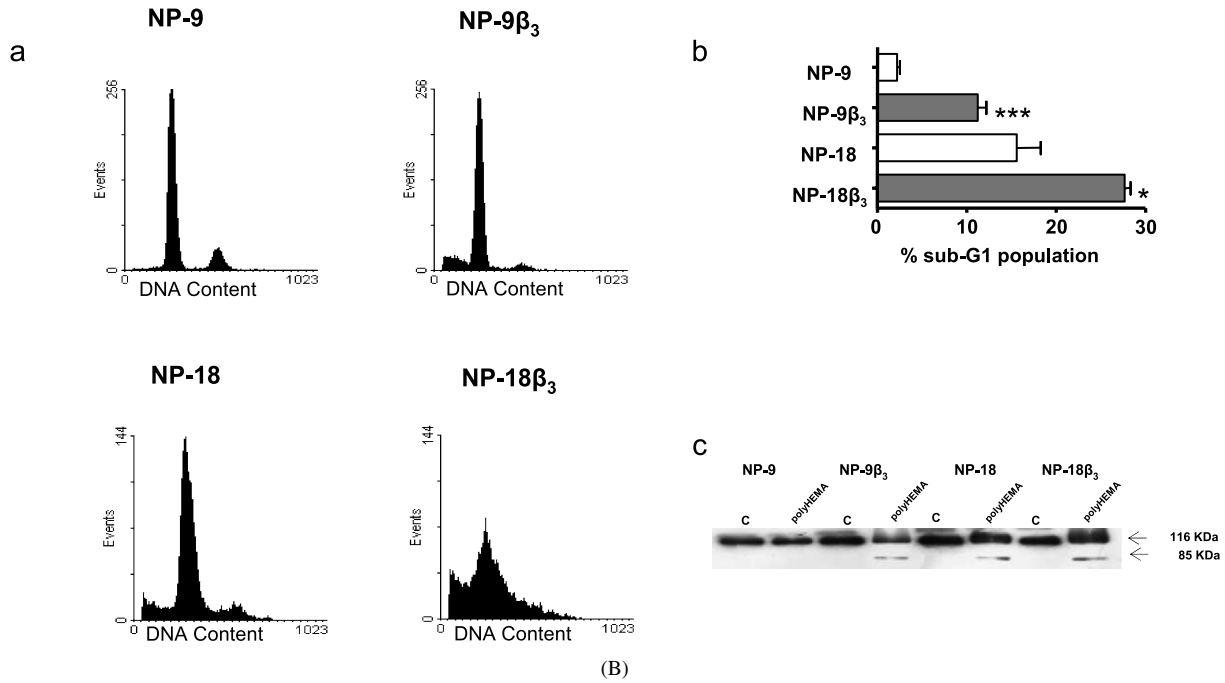

(B)

Fig. 5. (B) (a) Cell cycle profiles under non-attachment conditions. Cell cycle distribution was assessed by flow cytometry analysis of propidium iodide-stained cells on days 4 (NP-18 and NP-18β_3) and 7 (NP-9 and NP-9β_3) after seeding on poly-HEMA coats. (b) Quantification of the sub-G_1 peak was performed using WinMDI/Multicycle software. (c) Apoptosis under anchorage-independent conditions. Cleavage of poly(ADP-ribose)-polymerase (PARP) was assessed by Western blot detection of the 85 KDa cleaved form of PARP. C – standard conditions; polyHEMA – poly-HEMA coating.

pro-migratory effect exerted by β_3 may be partially compensated by high p16 levels. Notably, unlike NP-9, NP-18 cells maintain p16 expression. In this context, we show that β_3-overexpressing NP-18 cells exhibit a marked increase in p16 protein levels that could modulate $\alpha_5\beta_1$ levels and cell migration.

Analysis of the expression levels of other cell cycle proteins revealed increased CDK1 and p27 levels in NP-9β_3. However, these changes did not lead to modification of the cell cycle profiles or proliferation rates, suggesting that increases in p27 and CDK1 are associated with activities other than cell proliferation. Intriguingly, both proteins have been linked to cell migration by other authors. CDK1 is a cell migration promoter acting as a downstream effector of $\alpha_v\beta_3$ integrin [26]. In the cytoplasm, p27 is reported to regulate cytoskeletal structure and cell migration by directly interfering with the interactions between RhoA and its activators [5]. These findings are consistent with the increased cell migration observed in NP-9β_3. As shown in this study, the increased migration rate correlates with a decrease in RhoA activity, and is concomitant with higher p27 and CDK1 protein levels. The involvement of p27 and CDK1 in modulation of migration requires cytoplasmic localization. Immunolocalization analysis of CDK1 and p27 in NP-9 and NP-9β_3 cell lines confirms their presence in both the nucleus and cytoplasm, supporting a role in modulating cell migration, at least in NP-9β_3 cells. In addition, this cell line displays the fastest migration rate, reinforcing the correlation between $\alpha_v\beta_3$ overexpression and increased invasive behavior reported for different tumors [40].

The integrin $\alpha_v\beta_3$ can induce apoptosis upon disruption of cell–matrix contact [24,41]. Our experiments with poly-HEMA revealed a significant increase in anoikis in association with overexpression of β_3, being particularly remarkable the anoikis achieved in NP-18β_3 cells. This finding provides new evidence on the negative contribution of $\alpha_v\beta_3$ to the growth under anchorage-independent conditions. Moreover, given that the observed levels are particularly significant in NP-18β_3 cells, this result may be related to the increase in p16, and is consistent with anoikis induced in pancreatic models by overexpression of p16 via $\alpha_5\beta_1$ [28].

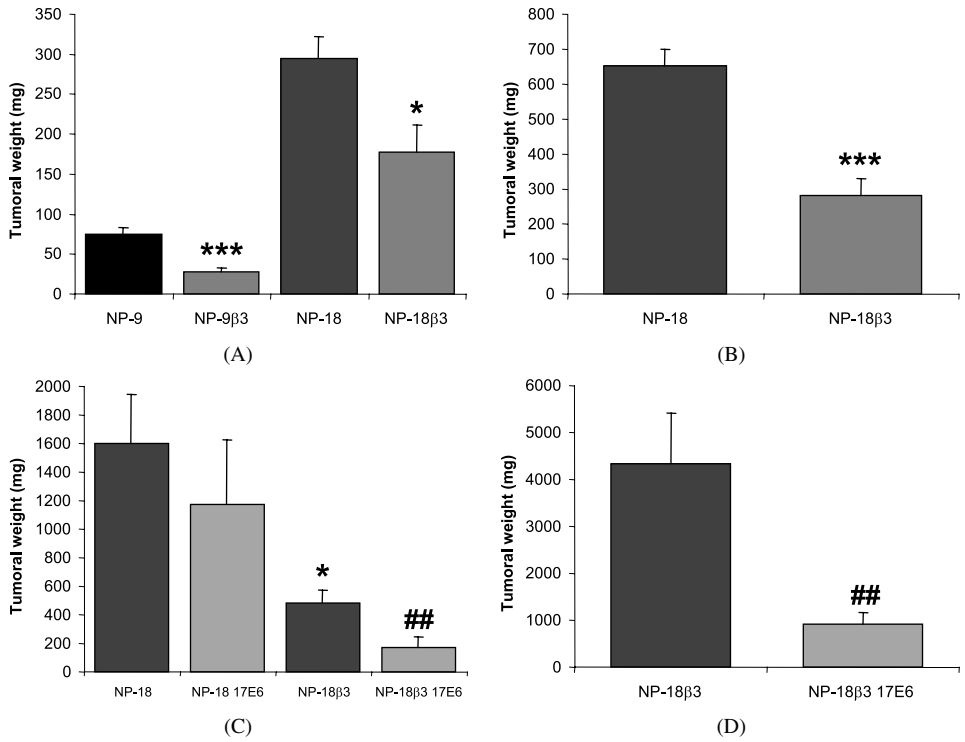

Fig. 6. Tumor growth and treatment with the 17E6 antibody. (A) Tumor growth into subcutaneous tissue. A total of 12×10^6 NP-9 or NP-9β_3 and 5×10^6 NP-18 or NP-18β_3 tumor pancreatic cells were injected subcutaneously into each posterior flank region of BALB/c *nu/nu* mice. After sacrifice, tumors were extracted and weighed. Bars represent means $\pm$ SD of tumor weights from 6–8 mice/condition. Statistics: t-test, $^*p \leqslant 0.05$, NP-18 vs. NP-18β_3 $^{***}p \leqslant 0.001$ NP-9 vs. NP-9β_3. (B) Tumor growth into pancreas. After 5 weeks of implantation of 10 mg tumor fragments by subcostal laparatomy, animals were sacrificed. Tumors were extracted and weighted. Bars represent means $\pm$ SD of tumor weights from 4–7 mice/condition. Statistics: t-test, $^{***}p \leqslant 0.001$ NP-18 vs. NP-18β_3. (C) Effects of 17E6 on subcutaneous tumors. Cells were injected s.c. in nude mice, as described for A. The mAb, 17E6 (1 mg/animal), or PBS were administered three times per week over six weeks from the first day. Next, animals were sacrificed and tumor weights determined. Bars show means $\pm$ SD of tumor weights from 4–6 mice/condition. Statistics: t-test, $^*p \leqslant 0.05$ untreated NP-18 vs. untreated NP-18β_3, $^{\#\#}p \leqslant 0.01$ untreated NP-18β_3 vs. 17E6-treated NP-18β_3. (D) Effects of 17E6 on intrapancreatic tumors. Tumor fragments were implanted in mouse pancreas, as described for (B). The mAb, 17E6 (500 μg/animal), or an equal volume of PBS was administered three times per week over 7 weeks from the seventh day after implantation. Next, animals were sacrificed and tumor weights determined. Bars depict means $\pm$ SD of tumor weights from 5–8 mice/condition. Statistics: t-test, $^{\#\#}p \leqslant 0.01$ untreated NP-18β_3 vs. 17E6-treated NP-18β_3.

β_3 overexpression leads to a significant reduction in the tumor growth rate in both subcutaneous and orthotopic models, evidencing that other factors, additional to the interaction with the intrapancreatic environment, play role in this growth suppression. This result is in line with observations in other tumors, such as glioma, in which β_3 overexpression does not affect *in vitro* growth, but reduces *in vivo* tumor formation [22, 23]. These findings are consistent with the behavior of KO mice [32], supporting dual roles of $\alpha_v\beta_3$ integrin [21]. The negative contribution of β_3 to *in vivo* growth suggests that the use of anti-α_v antibodies in therapies for pancreatic cancer might be contraindicated. Interestingly, 17E6 treatment reduced β_3-overexpressing tumor growth to a more significant extent, compared to those developed from parental cells. These data may be explained by the hypothesis formulated by Hynes that blocking reagents act as agonists of the negative regulatory function of α_v integrins [21].

Our results collectively show that β_3 expressed in pancreatic cancer cells exerts different effects, such as promotion of cell migration in monolayer cultures, induction of anoikis *in vitro*, and suppression of *in vivo* tumor growth, providing new evidence for involvement of the cell environment in the dual roles of $\alpha_v\beta_3$ integrin. Further studies with these models may aid in clarifying the factors that modulate $\alpha_v\beta_3$ integrin roles and establishing how pancreatic tumors respond when their integrin patterns are altered, eventually allowing bet-

ter prediction of the effects of therapeutic antitumoral agents applied to regulate integrin actions.

Aknowledgements

We are grateful to Merck and Dr. Stephanie Cambier for the monoclonal antibodies and Dr. Marshall for the pBabe/β_3 vector. We thank Drs. E. Danen, A. Sonnenberg and J. Collard for materials gift, critical comments, and generous help in pull-down assays, and J. Comas for his technical assistance at flow cytometry service. This research was supported by Ministerio de Ciencia e Innovación (Grants BIO2005-08682-C03-03 and BIO2008-04692-C03-03 to AM). SM and AV are recipients of predoctoral fellowships from Generalitat de Catalunya.

References

[1] A. Abdollahi, D.W. Griggs, H. Zieher, A. Roth, K.E. Lipson, R. Saffrich, H.J. Grone, D.E. Hallahan, R.A. Reisfeld, J. Debus, A.G. Niethammer and P.E. Huber, Inhibition of alpha(v)beta3 integrin survival signaling enhances antiangiogenic and antitumor effects of radiotherapy, *Clin. Cancer Res.* **11** (2005), 6270–6279.

[2] Y. Adachi, S.S. Lakka, N. Chandrasekar, N. Yanamandra, C.S. Gondi, S. Mohanam, D.H. Dinh, W.C. Olivero, M. Gujrati, T. Tamiya, T. Ohmoto, G. Kouraklis, B. Aggarwal and J.S. Rao, Down-regulation of integrin alpha(v)beta(3) expression and integrin-mediated signaling in glioma cells by adenovirus-mediated transfer of antisense urokinase-type plasminogen activator receptor (uPAR) and sense p16 genes, *J. Biol. Chem.* **276** (2001), 47171–47177.

[3] S.M. Albelda, S.A. Mette, D.E. Elder, R. Stewart, L. Damjanovich, M. Herlyn and C.A. Buck, Integrin distribution in malignant melanoma: association of the beta 3 subunit with tumor progression, *Cancer Res.* **50** (1990), 6757–6764.

[4] E. Alhaja, J. Adan, R. Pagan, F. Mitjans, M. Cascallo, M. Rodriguez, V. Noe, C.J. Ciudad, A. Mazo, S. Vilaro and J. Piulats, Anti-migratory and anti-angiogenic effect of p16: a novel localization at membrane ruffles and lamellipodia in endothelial cells, *Angiogenesis* **7** (2004), 323–333.

[5] A. Besson, M. Gurian-West, A. Schmidt, A. Hall and J.M. Roberts, p27Kip1 modulates cell migration through the regulation of RhoA activation, *Genes Dev.* **18** (2004), 862–876.

[6] M.F. Burbridge, V. Venot, P.J. Casara, F. Perron-Sierra, J.A. Hickman and G.C. Tucker, Decrease in survival threshold of quiescent colon carcinoma cells in the presence of a small molecule integrin antagonist, *Mol. Pharmacol.* **63** (2003), 1281–1288.

[7] G. Capella, L. Farre, A. Villanueva, G. Reyes, C. Garcia, G. Tarafa and F. Lluis, Orthotopic models of human pancreatic cancer, *Ann. New York Acad. Sci.* **880** (1999), 103–109.

[8] N. Cordes, Integrin-mediated cell–matrix interactions for prosurvival and antiapoptotic signaling after genotoxic injury, *Cancer Lett.* **242** (2006), 11–19.

[9] E.H. Danen and A. Sonnenberg, Integrins in regulation of tissue development and function, *J. Pathol.* **201** (2003), 632–641.

[10] E.H. Danen, P. Sonneveld, C. Brakebusch, R. Fassler and A. Sonnenberg, The fibronectin-binding integrins alpha5beta1 and alphavbeta3 differentially modulate RhoA-GTP loading, organization of cell matrix adhesions, and fibronectin fibrillogenesis, *J. Cell Biol.* **159** (2002), 1071–1086.

[11] E.H. Danen, J. van Rheenen, W. Franken, S. Huveneers, P. Sonneveld, K. Jalink and A. Sonnenberg, Integrins control motile strategy through a Rho-cofilin pathway, *J. Cell Biol.* **169** (2005), 515–526.

[12] J.S. Desgrosellier, L.A. Barnes, D.J. Shields, M. Huang, S.K. Lau, N. Prevost, D. Tarin, S.J. Shattil and D.A. Cheresh, An integrin alpha(v)beta(3)-c-Src oncogenic unit promotes anchorage-independence and tumor progression, *Nat. Med.* **15** (2009), 1163–1169.

[13] M.S. Duxbury, H. Ito, S.W. Ashley and E.E. Whang, c-Src-dependent cross-talk between CEACAM6 and alphavbeta3 integrin enhances pancreatic adenocarcinoma cell adhesion to extracellular matrix components, *Biochem. Biophys. Res. Commun.* **317** (2004), 133–141.

[14] R. Fahraeus and D.P. Lane, The p16(INK4a) tumour suppressor protein inhibits alphavbeta3 integrin-mediated cell spreading on vitronectin by blocking PKC-dependent localization of alphavbeta3 to focal contacts, *EMBO J.* **18** (1999), 2106–2118.

[15] S.M. Frisch and E. Ruoslahti, Integrins and anoikis, *Curr. Opin. Cell Biol.* **9** (1997), 701–706.

[16] M.Z. Gilcrease, Integrin signaling in epithelial cells, *Cancer Lett.* **247** (2007), 1–25.

[17] J.J. Grzesiak, J.C. Ho, A.R. Moossa and M. Bouvet, The integrin-extracellular matrix axis in pancreatic cancer, *Pancreas* **35** (2007), 293–301.

[18] D.S. Harburger and D.A. Calderwood, Integrin signalling at a glance, *J. Cell Sci.* **122** (2009), 159–163.

[19] R. Hosotani, M. Kawaguchi, T. Masui, T. Koshiba, J. Ida, K. Fujimoto, M. Wada, R. Doi and M. Imamura, Expression of integrin alphaVbeta3 in pancreatic carcinoma: relation to MMP-2 activation and lymph node metastasis, *Pancreas* **25** (2002), e30–e35.

[20] S. Huveneers, H. Truong and H.J. Danen, Integrins: signaling, disease, and therapy, *Int. J. Radiat. Biol.* **83** (2007), 743–751.

[21] R.O. Hynes, A reevaluation of integrins as regulators of angiogenesis, *Nat. Med.* **8** (2002), 918–921.

[22] M. Kanamori, S.R. Vanden Berg, G. Bergers, M.S. Berger and R.O. Pieper, Integrin beta3 overexpression suppresses tumor growth in a human model of gliomagenesis: implications for the role of beta3 overexpression in glioblastoma multiforme, *Cancer Res.* **64** (2004), 2751–2758.

[23] T. Kawaguchi, Y. Yamashita, M. Kanamori, R. Endersby, K.S. Bankiewicz, S.J. Baker, G. Bergers and R.O. Pieper, The PTEN/Akt pathway dictates the direct alphaVbeta3-dependent growth-inhibitory action of an active fragment of tumstatin in glioma cells *in vitro* and *in vivo*, *Cancer Res.* **66** (2006), 11331–11340.

[24] N.I. Kozlova, G.E. Morozevich, A.N. Chubukina and A.E. Berman, Integrin alphavbeta3 promotes anchorage-dependent apoptosis in human intestinal carcinoma cells, *Oncogene* **20** (2001), 4710–4717.

[25] K.R. Legate, S.A. Wickstrom and R. Fassler, Genetic and cell biological analysis of integrin outside-in signaling, *Genes Dev.* **23** (2009), 397–418.

[26] T. Manes, D.Q. Zheng, S. Tognin, A.S. Woodard, P.C. Marchisio and L.R. Languino, Alpha(v)beta3 integrin expression upregulates cdc2, which modulates cell migration, *J. Cell Biol.* **161** (2003), 817–826.

[27] A. Noguchi, N. Ito, H. Sawa, M. Nagane, M. Hara and I. Saito, Phenotypic changes associated with exogenous expression of p16INK4a in human glioma cells, *Brain Tumor Pathol.* **18** (2001), 73–81.

[28] T. Plath, K. Detjen, M. Welzel, Z. von Marschall, D. Murphy, M. Schirner, B. Wiedenmann and S. Rosewicz, A novel function for the tumor suppressor p16(INK4a): induction of anoikis via upregulation of the alpha(5)beta(1) fibronectin receptor, *J. Cell Biol.* **150** (2000), 1467–1478.

[29] X.D. Ren, W.B. Kiosses and M.A. Schwartz, Regulation of the small GTP-binding protein Rho by cell adhesion and the cytoskeleton, *EMBO J.* **18** (1999), 578–585.

[30] S.F. Retta, G. Cassara, M. D'Amato, R. Alessandro, M. Pellegrino, S. Degani, G. De Leo, L. Silengo and G. Tarone, Cross talk between beta(1) and alpha(V) integrins: beta(1) affects beta(3) mRNA stability, *Mol. Biol. Cell* **12** (2001), 3126–3138.

[31] A.R. Reynolds, L.E. Reynolds, T.E. Nagel, J.C. Lively, S.D. Robinson, D.J. Hicklin, S.C. Bodary and K.M. Hodivala-Dilke, Elevated Flk1 (vascular endothelial growth factor receptor 2) signaling mediates enhanced angiogenesis in beta3-integrin-deficient mice, *Cancer Res.* **64** (2004), 8643–8650.

[32] L.E. Reynolds, L. Wyder, J.C. Lively, D. Taverna, S.D. Robinson, X. Huang, D. Sheppard, R.O. Hynes and K.M. Hodivala-Dilke, Enhanced pathological angiogenesis in mice lacking beta3 integrin or beta3 and beta5 integrins, *Nat. Med.* **8** (2002), 27–34.

[33] A.J. Ridley, Rho GTPases and cell migration, *J. Cell Sci.* **114** (2001), 2713–2722.

[34] E. Sahai, Mechanisms of cancer cell invasion, *Curr. Opin. Genet. Dev.* **15** (2005), 87–96.

[35] R. Soldi, S. Mitola, M. Strasly, P. Defilippi, G. Tarone and F. Bussolino, Role of alphavbeta3 integrin in the activation of vascular endothelial growth factor receptor-2, *EMBO J.* **18** (1999), 882–892.

[36] C.H. Streuli, Integrins and cell-fate determination, *J. Cell Sci.* **122** (2009), 171–177.

[37] D. Taverna, D. Crowley, M. Connolly, R.T. Bronson and R.O. Hynes, A direct test of potential roles for beta3 and beta5 integrins in growth and metastasis of murine mammary carcinomas, *Cancer Res.* **65** (2005), 10324–10329.

[38] K. Tzukert, N. Shimony, L. Krasny, S. Urieli-Shoval, R. Gorodetsky, I. Avrahami, D.M. Nettelbeck and Y.S. Haviv, Human melanoma cells expressing the alphavbeta3 integrin are partially protected from necrotic cell death induced by dynamic matrix detachment, *Cancer Lett.* **290** (2010), 174–181.

[39] P. Villalonga and A.J. Ridley, Rho GTPases and cell cycle control, *Growth Factors* **24** (2006), 159–164.

[40] G.K. Wang and W. Zhang, The signaling network of tumor invasion, *Histol. Histopathol.* **20** (2005), 593–602.

[41] Y. Wu, J. Zuo, G. Ji, H. Saiyin, X. Liu, F. Yin, N. Cao, Y. Wen, J.J. Li and L. Yu, Proapoptotic function of integrin beta(3) in human hepatocellular carcinoma cells, *Clin. Cancer Res.* **15** (2009), 60–69.

[42] D.Q. Zheng, A.S. Woodard, M. Fornaro, G. Tallini and L.R. Languino, Prostatic carcinoma cell migration via alpha(v)beta3 integrin is modulated by a focal adhesion kinase pathway, *Cancer Res.* **59** (1999), 1655–1664.